Investigations of *p*-wave scattering of neutrons by nuclei

G. S. Samosvat

Fiz. Élem. Chastits At. Yadra **26**, 1567–1596 (November–December 1995)

The studies of the angular dependence of the scattering of neutrons with energies below ~0.3 MeV made at the I. M. Frank Laboratory of Neutron Physics in the period 1964–1993 are reviewed. A significant proportion of these studies were initiated by F. L. Shapiro. After a brief introduction devoted to Shapiro, seven sections of the review describe the results of investigations with p neutrons on: 1) estimating the neutron electric polarizability; 2) the energy and mass dependences of the forward–backward scattering asymmetry; 3) the determination of the mixtures of the spin channels in p resonances; 4) the first observation of the spin–orbit splitting of the $3p$ maximum of the neutron strength function; 5) the first systematic study of the p-wave scattering radii; 6) searches for the effect of one-pion exchange in p-wave scattering of neutrons by odd nuclei; 7) identification of negative p resonances. The prospects for further investigations are discussed in the final section.

It is true that the investigations into the p-wave interaction of neutrons with nuclei do not belong to the most eminent achievements of Fedor L'vovich Shapiro, which are honored in the present issue. Nevertheless, his ideas and influence were also decisive for many years in this field of neutron physics, in which his students and successors worked.

For the systematic study of the p-wave interaction, neutrons with energies from a few to hundreds of kilo-electron-volts are best suited. Shapiro and collaborators performed experiments with such neutrons at the P. N. Lebedev Physics Institute of the USSR Academy of Sciences, measuring the cross sections for radiative capture using the well-known "lead cube" by the method of neutron moderation in lead.[1] These experiments yielded much new information about the p-wave interaction, initially at individual resonances and later in the cross sections averaged over the resonances.

In numerous elements, including ones in important constructional materials, previously unknown resonances with very small neutron widths were discovered and solely on the basis of this property were identified as p-wave resonances. Subsequently, they were almost all confirmed. They included the "famous" resonance at 1180 keV in ^{56}Fe, the parity of which was long a matter of dispute, which was ended by the first direct identification of a p-wave resonance on the basis of the angular dependence of the scattering in Ref. 2.

Theoretical analysis of the averaged cross sections of the (n,γ) reaction showed[3] that with increasing neutron energy the contribution of s-wave capture decreases, the contribution of p-wave capture increases, and the cross section is determined by four parameters: the values of the radiative, $\overline{\Gamma}_\gamma/D_l$, and neutron, $\overline{\Gamma}^{(1)}/D_l = S_l$, strength functions for $l=0$ and 1. This made it possible to obtain a large set of values of S_l in the region of mass numbers around $A=90$, and this, in its turn, made it possible to eliminate some early "discoveries" of spin–orbit splitting of the $3p$ maximum of the neutron strength function.

At the time of completion of these studies at the Lebedev Institute—they were included in Shapiro's doctoral dissertation, forming in it only one small chapter (see Ref. 4)—an excellent source of kilo-electron-volt neutrons reached full power at Dubna. This was the pulsed fast reactor (IBR) and later its modification IBR-30 with and without electron injectors. Also developed at that time was the theoretical basis[5,6] for new studies with p-wave neutrons based on measurements of the angular dependence of the elastic scattering.

In what follows we shall discuss in chronological order the varied investigations of the p-wave interaction of neutrons with nuclei that were made at the I. M. Frank Laboratory of Neutron Physics at the JINR during the period 1964–1993. We mention that all these studies were more or less unique.

1. ESTIMATE OF THE NEUTRON POLARIZABILITY

It is well known that if an uncharged macroscopic body, containing electric charges of opposite signs, is placed in an electric field **E**, then it acquires an electric dipole moment $\mathbf{p}=\alpha\mathbf{E}$, i.e., the body is polarized. Exactly the same idea was advanced simultaneously and independently for a nucleon in the electromagnetic field of the photon[7] and for a neutron that enters the Coulomb field of a heavy nucleus.[8] The first searches for neutron polarizability were made by small-angle scattering of fast neutrons by nuclei (see the book of Ref. 9). Many experiments were made, and the interpretation of some of them led to a neutron polarizability $\alpha_n \sim 10^{-40}$ cm^3. However, it soon became clear that this was about 100 times greater than both the theoretical predictions and the analogous quantity for the proton. It was at this time that Thaler[10] proposed that experiments should be made in the kilo-electron-volt range of energies, in which the p-wave interaction is just beginning to have an effect, and in the expansion of the differential cross section with respect to Legendre polynomials[1)]

$$\sigma(\theta)=\sum_{i=0}^{\infty} B_i P_i(\cos\theta), \tag{1}$$

where θ is the scattering angle, only the first two or three terms are important. In the absence of resonances,

 1063-7796/95/060655-14$10.00

$$\sigma(\theta)=\frac{1}{k^2}(\sin^2\delta_0+6\sin\delta_0\sin\delta_1\cos(\delta_0-\delta_1)\cos\theta$$
$$+6\sin^2\delta_1 P_2(\cos\theta)), \quad (2)$$

where k is the neutron wave number, and δ_0 and δ_1 are the real phase shifts of the s and p waves, respectively. In the case of scattering by a short-range spherically symmetric potential, as the nuclear potential is,

$$\delta_l=\frac{(k\bar{R})^{2l+1}}{[(2l+1)!!]^2}C, \quad (3)$$

where the constant $C\simeq 1$ depends only on the specific form of the potential, and $\bar{R}$ is some effective radius of it. If (2) is represented in the form

$$\sigma(\theta)=\frac{\sigma_s}{4\pi}(1+\omega_1\cos\theta+\omega_2 P_2(\cos\theta)), \quad (4)$$

where $\sigma_s=4\pi\sin^2\delta_0/k^2$ is the integrated scattering cross section, then for the "visiting card" of the p-wave neutrons—the coefficient of the forward–backward scattering asymmetry—we obtain

$$\omega_1=\frac{6\sin\delta_1\cos(\delta_0-\delta_1)}{\sin\delta_0}\simeq\frac{6\delta_1}{\delta_0}\simeq\frac{2}{3}(k\bar{R})^2=\frac{4m}{3\hbar^2}\bar{R}^2E \quad (5)$$

(m is the mass of the neutron, and E is its energy). It can be seen from Eqs. (5) that at low energies, when δ_0, $\delta_1\ll 1$, the asymmetry of the nuclear scattering increases linearly with the neutron energy.

In accordance with the hypothesis of polarizability of the neutron, its scattering by a nucleus possessing charge Ze will be accompanied by additional phase shifts of the scattered waves due to the additional interaction of the induced moment $\mathbf{p}$ with the Coulomb field $\mathbf{E}$ of the nucleus:

$$V=-\frac{1}{2}\mathbf{pE}=-\frac{1}{2}\alpha_n E^2=-\frac{\alpha_n Z^2e^2}{2r^4}. \quad (6)$$

The potential (6) is small in magnitude compared with the nuclear potential but decreases with increasing neutron–nucleus separation r more slowly, and therefore p-wave scattering by such a potential must be damped more slowly with decreasing energy than is the case for the nuclear potential well. At small k, the phase-shift corrections calculated in the Born approximation are

$$\Delta\delta_0=\frac{6}{5}\left(\frac{Ze}{\hbar}\right)^2\frac{\alpha_n m}{R_N}k\left(1-\frac{5}{18}\pi kR_N+\frac{5}{21}(kR_N)^2-\ldots\right), \quad (7)$$

$$\Delta\delta_1=\left(\frac{Ze}{\hbar}\right)^2\frac{\alpha_n m}{R_N}k\left(\frac{\pi}{15}kR_N-\frac{2}{21}(kR_N)^2+\ldots\right), \quad (8)$$

where R_N is the radius of a uniformly charged ball that imitates the electric field of the nucleus. For heavy nuclei, one can set $R_N=1.20A^{1/3}$ F (Ref. 11). Adding (7) and (8) to the corresponding phase shifts in accordance with (3) and substituting the resulting sums in the first of the approximate equations (5), we readily see that at low energies the asymmetry ω_1 acquires the energy dependence

$$\omega_1=aE-bE^{1/2}, \quad (9)$$

in which a and b are positive constants, and

$$b=\frac{2\sqrt{2}\pi\alpha_n m^{3/2}e^2Z^2}{5\hbar^3\bar{R}}=3.03\cdot 10^{-7}\frac{\alpha_n Z^2}{R_0'}\ \text{keV}^{-1/2}. \quad (10)$$

The minus sign in front of b in (9) is a consequence of the fact that δ_1 and δ_0 are negative but $\Delta\delta_1$ is positive, and $|\delta_0|>\Delta\delta_0$. The numerical value of b in (10) corresponds to α_n taken in units of 10^{-42} cm^3 and range R_0' of the potential s-wave scattering measured in fermis.

The relations (2)–(10) were used in the already cited study of Thaler,[10] who analyzed the experimental values of the coefficient ω_1 for uranium in the range 30–300 keV and found that the asymptotic behavior of the curve (9) describing the data intersects the abscissa (if it does not pass through the origin) at a point distant not more than 20 keV. From this he found the limiting b and concluded that

$$\alpha_n<20\cdot 10^{-42}\ \text{cm}^3. \quad (11)$$

The first attempt to improve this estimate was made at the Laboratory of Neutron Physics in 1964.[12] By means of a detector of scattered neutrons (BF_3 counters of total volume ~3 liter) that could be displaced in its angular position and was situated 100 m from the IBR reactor, five values of ω_1 with errors 0.01–0.02 were obtained for Pb nuclei in the interval 0.5–7.5 keV. This demonstrated the possibility of experimenting with p-wave neutrons and of lowering the limit (11) for the polarizability by increasing the range of neutron energies and raising the statistical accuracy of the measurements of ω_1.

About a year later, an experimental facility with flight path 250 m, as shown schematically in Fig. 1, had been constructed. A collimated neutron beam with section measuring 12×22 cm^2 was incident on a hollow lead cylinder of height 20 cm with outer and inner diameters 10 and 8 cm, respectively. The scattered neutrons were detected by nine detectors placed at angles from 30° to 150° relative to the incident beam. Each detector was a battery of 20 proportional counters of SNMO-5 type filled with BF_3 gas enriched with the isotope ^{10}B. The detectors were surrounded on all sides by a cadmium layer of thickness 1–2 mm and were in a massive shield of paraffin and boron carbide. On both sides of the sample, the neutron beam passed through an argon atmosphere contained in a tube of diameter 45 cm made of thin polyethylene.

The background was taken into account by alternating the measurements with the sample in the beam and outside the beam, and this was found to be fairly accurate. The observed angular distributions were carefully corrected. Corrections were made for distortions arising as a result of the following: 1) the change in the neutron energy as a result of the scattering; 2) the small differences of the spectral sensitivities of the different detectors; 3) the appreciable thickness of the scatterer and the effect of self-screening and multiple scattering. At all energies, the corrected distributions were normalized to one and the same distribution at the low mean energy $E_0=0.25$ keV. This procedure reduced the effect of all

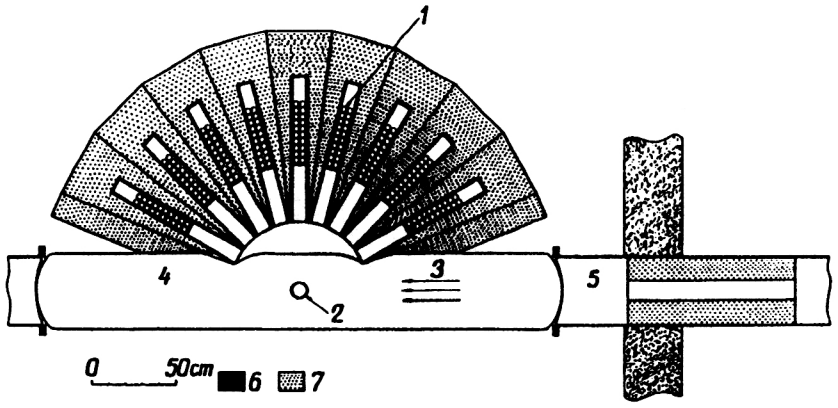

FIG. 1. Horizontal section of the measuring facility: 1) detector; 2) sample; 3) incident beam; 4) argon atmosphere; 5) vacuum neutron guide with collimator; 6) B_4C; 7) paraffin with B_4C.

the corrections, the differences of the detectors, and the drift of the apparatus, and the distributions themselves became proportional to $\sigma(\theta)$ in the center-of-mass system. The results were analyzed for 11 energy intervals. The effective energy of each interval was found by integrating over the time of flight with allowance for the resolution function (the neutron burst was a Gaussian curve with half-width 60 μs), the neutron spectrum, and the energy sensitivity of the detectors. The anisotropy parameters ω_1 and ω_2 in the expression (4) were found from the observed angular dependences of the scattering by the least-squares method.

Further, with allowance for the normalization to the energy E_0 and the values obtained for ω_1, the fitting was done, not on the basis of (9), but according to the formula

$$\omega_1 = a(E-E_0) - b(E^{1/2}-E_0^{1/2}),$$

and this led to the coefficients $a=(1.91\pm0.42)\cdot10^{-3}$ keV^{-1} and $b=(0.07\pm1.96)\cdot10^{-3}$ keV$^{-1/2}$ and, in accordance with (10) for $R_0' = 9.5$ F, to the polarizability

$$\alpha_n = (0.3\pm9.2)\cdot10^{-42}\ \text{cm}^3.$$

A more accurate estimate is obtained by a joint analysis with the data for ω_1 for lead from Ref. 13. Addition of the six points for ω_1 in the range $E=50$–160 keV gave $a=(1.92\pm0.20)\cdot10^{-3}$ keV^{-1}, $b=(0.15\pm1.16)\cdot10^{-3}$ keV$^{-1/2}$, and

$$\alpha_n = (0.7\pm5.4)\cdot10^{-42}\ \text{cm}^3. \qquad (12)$$

Figure 2 illustrates this result and also shows the curve for $\omega_1(E)$ corresponding to the limit (11) from Ref. 10.

The estimate (12) published in Ref. 14 remained the record until 1988, when the use of high-precision measurements of the total neutron cross section enabled the experimentalists to advance to a level of accuracy of α_n of the order of $1\cdot10^{-42}$ cm^3.

2. MASS DEPENDENCE OF THE SCATTERING ASYMMETRY

For about the next three years, the same facility (see Fig. 1) was used to make approximately the same measurements as in the case of Pb for a further nine elements: Sr, Mo, Rh, Cd, Sn, Sb, Te, I, La, Th. The aim of these investigations was to establish the behavior of ω_1, i.e., of the relative contribution of the p-wave neutrons to the scattering, as a function of the neutron energy E and the mass number A of the nucleus. There were two differences between these measurements and the first ones. First, an accuracy of ω_1 as high as in the case of lead was not required, and this made the problem easier. Second, all the nuclei except for Pb have many resonances in the studied region of energies, and this made the problem more complicated—it was necessary to establish their effect on the measured ω_1.

All the samples had the natural isotopic composition and weighed between 1.8 and 6.6 kg; they had the form of either a hollow or solid cylinder or a flat plate. In the last case, the sample was placed at an angle to the beam that coincided with the angle of one of the detectors, the counts from which were not taken into account in the analysis in view of the strong distortions.

The measured values of ω_1 (in the center-of-mass system) as functions of the neutron energy (in the laboratory system) are shown in Fig. 3. It can be seen that they have a tendency to increase linearly with the energy for all the ele-

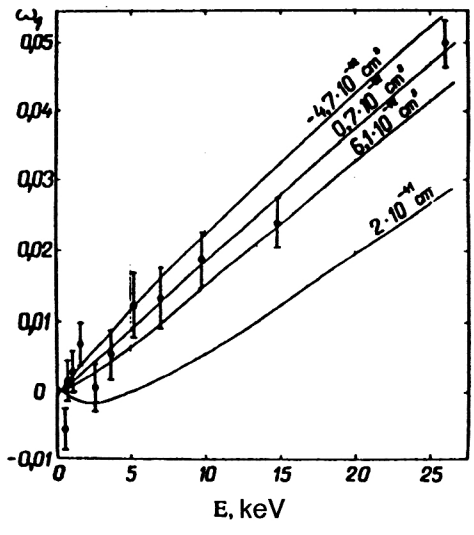

FIG. 2. Experimental values of ω_1 for lead from Ref. 14. The curves were calculated for $a=1.92\cdot10^{-3}$ keV^{-1} and the indicated values of α_n.

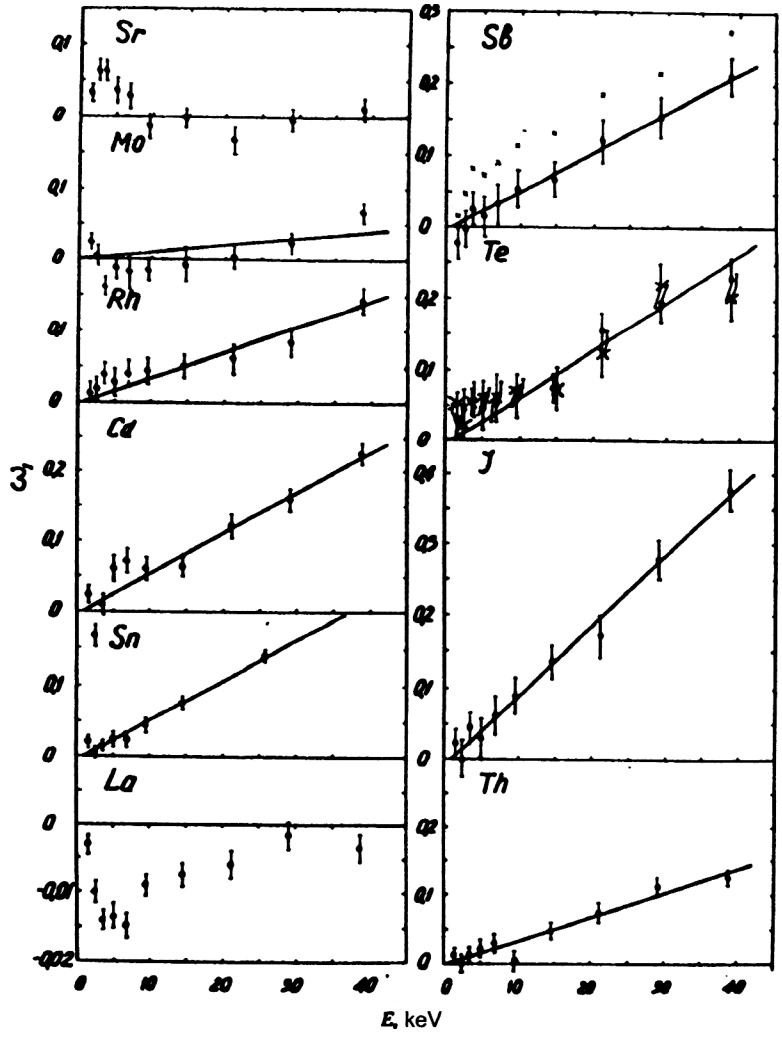

FIG. 3. Experimental values of ω_l (Refs. 15 and 16). The crosses for Sb are the values of ω_l uncorrected for the self-screening effect in the thick sample; the open symbols for Te are the results of the measurements with the filter.

ments except La and, possibly, Sr. It became clear later that the lanthanum "anomaly" was a consequence of three circumstances: the presence in the metal of a few atomic percent of hydrogen, the strong variation of the integrated cross section of lanthanum, and the normalization of all the angular distributions to the distribution at $E_0 \approx 0.8$ keV. The proportionality of ω_l to the energy E for all samples except for La and Sr is demonstrated in the figure by the fitted straight lines passing through the energy E_0. It can be assumed that the rate of increase of ω_l with increasing E, which is characterized by the derivative $d\omega_l/dE$, is a constant equal to ω_l/E for the majority of the nuclei. The experimental values of this constant are given in Fig. 4 as a function of the mass number A (black circles). The open circles in the same figure give the estimates of ω_l/E from the data for $E>30$–60 keV compiled in Ref. 13.

A first, very rough estimate of the dependence of ω_l/E on A can be obtained from the last approximate equation (5) by taking as effective radius of the potential well, say, $\bar{R}=1.25A^{1/3}$ F. Then $\omega_l/E=0.0504A^{2/3}$ MeV^{-1}, as shown by the dot–dash curve in Fig. 4. It is evident that this estimate is no better founded than, for example, the estimate by a constant 10^{-4} of the neutron strength functions in the model of a "black" nucleus. It is obvious that we are here dealing with a combination of "size resonances" for s- and p-wave scattering and that for a more adequate description a model of a "semitransparent" nucleus is required.

For the correct comparison with the optical model, at least two conditions must be satisfied: good averaging over the states of the compound nucleus and the possibility of obtaining the compared quantity from an S matrix that can be calculated in the model. In our case, the first condition is well satisfied for $E \geqslant 10$ keV, since the width of the energy resolution function at these energies is many times greater than the interresonance separations of all the investigated nuclei except Pb. The fulfillment of the second condition is established in detail in Refs. 15 and 16, and in the comparison of the experimental values of ω_l with the values calculated in the optical model there is no need to take into account a contribution to ω_l from the compound-nucleus resonances.

By averaging the Breit–Wigner expressions written down for the differential cross section (see Refs. 15 and 17)

with respect to the energy it was shown that the s-wave resonances decrease, and the p resonances increase, the "potential" ω_l and that the magnitudes of these changes can be expressed in terms of the known cross sections and strength functions. The most significant decrease of ω_l (by about 30%) at $E=40$ keV should have occurred for Te but did not, as can be seen from Fig. 3. In the figure, the open circles, which completely coincide with the black circles, show the results of the measurements made when a tellurium filter of thickness 0.045 nucleus/b, which appreciably depleted the beam of resonance neutrons, was placed in the beam. Thus, the effect of the blocking of the resonances in the thickest scatterers made it possible to avoid having to use corrections for the resonances, and the calculations in the optical model could be directly compared with the observed ω_l.

The calculations were made with a spherical potential of standard shape for which the best values of its parameters were found by the least-squares method. The data used in the fitting included in each case the values of ω_l/E, about 20 "typical" experimental values of the strength function S_0, the radius R_0' of the potential scattering, and the total cross section σ_t at $E=40$ keV. The form of the potential, the obtained parameter sets, and other details can be found in Refs. 15 and 16. Here we give only the expression for the constant ω_l/E in terms of the elements η_{lj} of the optical S matrix:

$$\frac{\omega_l}{E}=\frac{2}{E}\cdot\frac{(\mathrm{Re}\ \eta_{0\,1/2}-1)(2\,\mathrm{Re}\ \eta_{1\,3/2}+\mathrm{Re}\ \eta_{1\,1/2}-3)+\mathrm{Im}\ \eta_{0\,1/2}(2\,\mathrm{Im}\ \eta_{1\,3/2}+\mathrm{Im}\ \eta_{1\,1/2})}{(\mathrm{Re}\ \eta_{0\,1/2}-1)^2+(\mathrm{Im}\ \eta_{0\,1/2})^2},$$

where $j=l\pm 1/2$ is the total angular momentum of the neutron; the contributions of the partial waves with $l>1$ and also of the terms containing $\eta_{1\,3/2}-\eta_{1\,1/2}$ are here ignored.

The results of the calculations are shown in Fig. 4 by the three curves labeled I, II, and M, which correspond to three different sets of numerical values of seven or eight parameters of the potential. The parameter set I was obtained when only the values of S_0, R_0', and σ_t were fed into the computer. In the first stages of the fitting, up to five parameters were varied simultaneously, and by degrees their number was reduced to one. Set II was obtained when only information about ω_l/E was used and the values of the parameters in set I were employed as initial values. The parameters were varied in the same sequence, this being such that there is a growth of their effect on the value of ω_l/E. Finally, the set M corresponds to the Moldauer potential of Ref. 18 fitted to the data on S_0, σ_t, and $\sigma(\theta)$ at energies 0.4–1 MeV in the range of mass numbers from 40 to 150. Naturally, potential II reproduces better than the others the main features in the behavior of ω_l/E as a function of the mass of the nucleus, while globally, judging from the values of χ^2, all three potentials describe the complete set of data with approximately the same success.

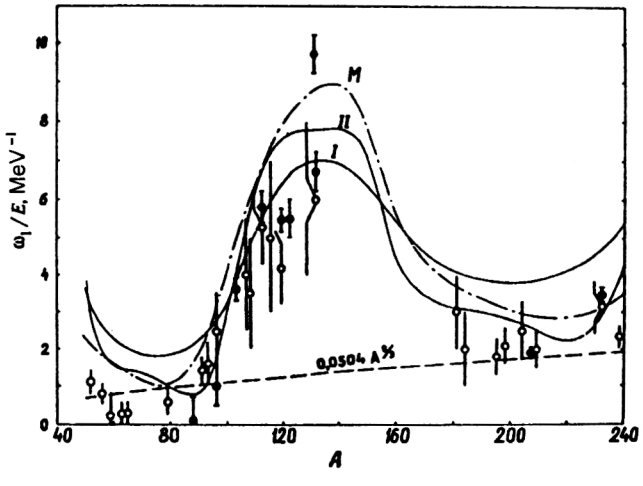

FIG. 4. Values of ω_l/E as a function of the mass number of the nucleus. The curves are the results of optical-model calculations.

Thus, for the data on the asymmetry of the scattering of kilo-electron-volt neutrons the optical model gives a description of the same nature as for the other data on the interaction of neutrons with nuclei.

3. DETERMINATION OF SPIN-CHANNEL MIXTURES

The initiator of the investigations that are described below was F. L. Shapiro; in his lectures of Ref. 6, he not only proposed the idea of the experiments but also convincingly justified his prediction of their results.

In accordance with the rules for adding angular momenta, p-wave resonances having total spin $J=I\pm 1/2>0$ are formed on target nuclei with spin $I\neq 0$ in two different ways, or channels:

$$\mathbf{J}=\mathbf{I}+\frac{\mathbf{1}}{\mathbf{2}}+\mathbf{1}=\begin{cases}I+1/2+0\\ I-1/2+1\end{cases}=I+1/2\qquad\qquad\begin{cases}I+1/2-1\\ I-1/2+0\end{cases}=I-1/2, \tag{13}$$

which are characterized by channel spins $s=I+1/2$ or $I-1/2$. Accordingly, the neutron widths of such resonances also contain two components:

$$\Gamma_n=\Gamma_{n+}+\Gamma_{n-}=(1-\beta)\Gamma_n+\beta\Gamma_n,\quad \beta=\Gamma_{n-}/\Gamma_n, \tag{14}$$

where we call β the channel-mixing parameter.[2)]

The question naturally arises of whether Γ_{n+} and Γ_{n-} fluctuate from resonance to resonance independently or are correlated. Shapiro answered this question as follows:[6] "The amplitude of the neutron width is proportional to a certain overlap integral between the wave function Ψ_λ of the given

resonance state of the compound nucleus and the wave function φ_s of the system consisting of the neutron and the original nucleus:

$$\gamma_s \sim \int \Psi_\lambda \varphi_s d\tau.$$

The wave functions that correspond to the same spin and parity values but different energy values are mutually orthogonal. Therefore, the thousands of functions Ψ_λ for different resonances λ are mutually orthogonal. This means that the Ψ_λ are very complicated functions, indeed so complicated that the overlap integral with any function φ is very small and fluctuates randomly around zero in going from resonance to resonance. The functions φ_{s_1} and φ_{s_2} for two spin channels are mutually orthogonal, i.e., differ fairly strongly from one another. Therefore, there are no grounds for expecting their overlap integrals with Ψ_λ to be correlated. It is to be expected that γ_{s_1} and γ_{s_2} will fluctuate independently of each other around the zero value." A detailed theoretical analysis of the correlations between the channels was made by Lane.[19] He showed that under the conditions for which the "standard" statistical model is valid there should not be any correlations between any pairs of channels.

If the reduced widths $\Gamma_{n+}^{(1)}$ and $\Gamma_{n-}^{(1)}$ fluctuate independently in accordance with the Porter–Thomas distribution, then for the distribution of the parameter β we can obtain the expression

$$P(\beta)d\beta = \frac{\sqrt{x}}{\beta + x(1-\beta)} \cdot \frac{d\beta}{\pi\sqrt{\beta(1-\beta)}}, \qquad (15)$$

where $x = \langle\Gamma_{n-}^{(1)}\rangle / \langle\Gamma_{n+}^{(1)}\rangle$, from which it follows that the mean value is $\langle\beta\rangle = \sqrt{x}/(1+\sqrt{x})$. For equal mean reduced widths in the two channels ($x=1$), the mean value is $\langle\beta\rangle = 0.5$, and the distribution is symmetric about $\beta = 0.5$. Only a difference of the mean values $\langle\Gamma_{n+}\rangle$ and $\langle\Gamma_{n-}\rangle$ by a factor 10 shifts $\langle\beta\rangle$ to 0.76 or 0.24. A characteristic feature of the distribution (15) is the concentration of the values of β near 0 or 1 [$P(\beta) \to \infty$ as $\beta \to 0$ and 1] for any finite ratio of the mean widths $x > 0$.

For the separate determination of the partial widths Γ_{n+} and Γ_{n-}, it is necessary to measure at the resonance the angular distribution of the scattered neutrons[6,20] or the γ rays of radiative capture,[21,22] or to work with polarized neutrons and (or) nuclei.[6,22,23] Before the investigations at the Laboratory of Neutron Physics, the first method had been tested only once[20] and had given practically no information about the spin channels, while the second and third methods had given only results for individual resonances, saying nothing about the distribution of β.

As was shown in Ref. 24, the parameter β can be determined by measuring at two different scattering angles the area of the p-wave resonance under the scattering curve. This area has the dependence[3)]

$$B(\theta) = B_0[1 + \omega_2 P_2(\cos\theta)], \qquad (16)$$

where for the investigated nuclei with spin $I = 1/2$ the anisotropy coefficient takes values that depend on the spin of the resonance:

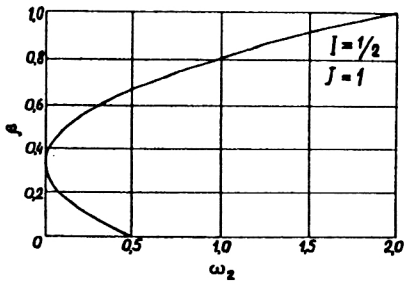

FIG. 5. Dependence of β on ω_2 for $I = 1/2$, $J = 1$.

$$\omega_2 = \begin{cases} 0 & \text{for } J=0, \\ \frac{1}{2}(3\beta-1)^2 & \text{for } J=1, \\ 7/10 & \text{for } J=2. \end{cases} \qquad (17)$$

Thus, if the measured ω_2 differs from 0 and 0.7, then the spin of the resonance is uniquely determined to be $J = 1$, and the mixture β of its spin channels is not entirely uniquely determined. The connection between β and ω_2 is shown in Fig. 5.

The experiments to study the spin channels, like all the other experiments described below, were already made using the IBR-30 operated in the booster regime and giving neutron pulses with half-width of about 4.5 μs and repetition frequency 100 Hz. The experimental arrangement with a 250-m flight path shown schematically in Fig. 6 was used. The most important part of the facility—the detector of the scattered neutrons—was a battery of ^{3}He counters having a gas pressure of about 10 atm and total working volume ~8 liter. The accessible range of angles was ~35°–145° with maximum uncertainty ±10°, and the solid angle was $\Omega/4\pi \approx 6 \cdot 10^{-3}$. The spectral efficiency of the detector was approximately (E is measured in electron volts)

$$\varepsilon(E) = \begin{cases} 1 - e^{-2.6/\sqrt{E}} & \text{for } E < 50 \text{ eV}, \\ 1.12E^{-0.33} & \text{for } E > 50 \text{ eV}. \end{cases}$$

In order to determine ω_2 from Eq. (16), it is necessary to measure the area of the resonance at two angles. In practice,

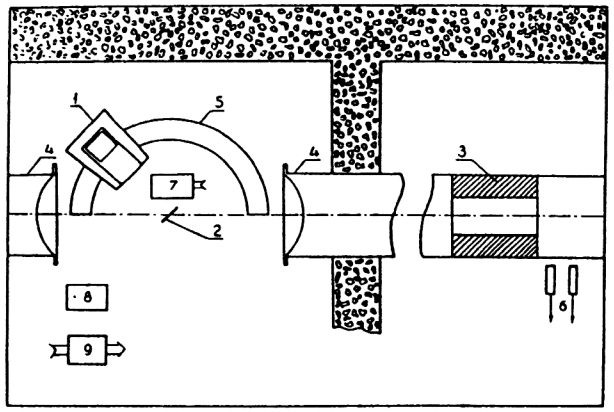

FIG. 6. Schematic arrangement of the facility with 250-m flight path: 1) detector in shield; 2) sample; 3) collimator; 4) vacuum neutron guide; 5) fixed platform of detector; 6) monitor counters; 7) electromechanical drive for displacing the detector and sample; 8) detector electronics; 9) drive control block.

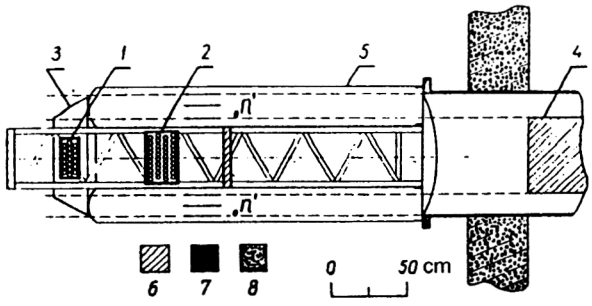

FIG. 7. Schematic arrangement of the facility with 1000-m flight path: 1) detector at 90°; 2) detector at 150°; 3) sample; 4) collimator; 5) polyethylene bag; 6) paraffin with B_4C; 7) B_4C; 8) concrete.

the detector was placed at angle 90° and at an angle close to 35° or 145°, and the flat sample was positioned perpendicular to the bisector of the angle between the pair of chosen scattering directions.

For a 1000-m flight path, a different arrangement, shown in Fig. 7, was used. The neutron beam, which had in section the shape of a ring with diameters 80 and 60 cm, passed through an argon atmosphere and was scattered by an annular sample of conical shape. The neutrons scattered through angles of about 90° and 150° were detected by two batteries of ^{3}He counters.

Three experiments were performed: initially, two with flight base 250 m, and then one with base 1000 m. The first experiment was performed with samples of metallic yttrium measuring 20×19 cm^2 and having weight 284 and 554 g. An example of the spectra of the scattered neutrons is shown in Fig. 8; they are normalized with respect to monitors but for convenience are displaced by 500 counts. The curves are the result of fitting a smooth background and peaks of standard shape. The arrows indicate the positions, in kilo-electron-volts, of the known resonances (the open circles are for the s-wave resonances, and the black circles for the p-wave resonances); the lengths of the arrows are proportional to the

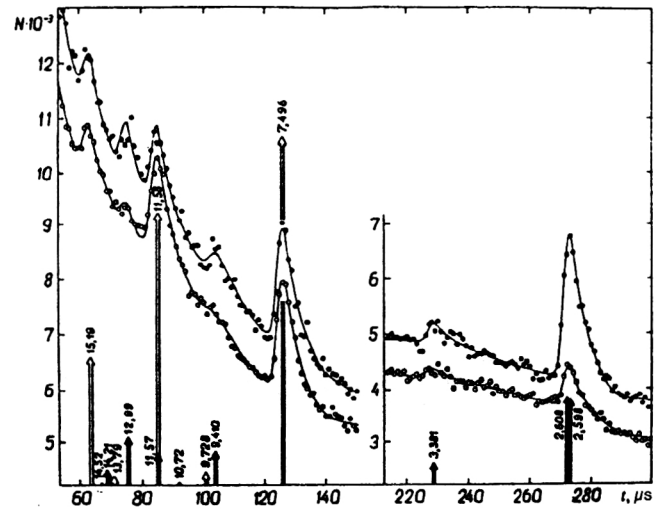

FIG. 8. Example of scattering spectra at the angles 90° (open symbols) and 143° (black symbols) for a thin ^{89}Y sample. The number of counts in the channel is N, and t is the number of a channel of width 1 μs.

calculated areas B_0 of the resonances in (16). The result of this investigation[24] was the determination of three or four mixtures of spin channels, all with approximately the same value $\beta \simeq 0.8$.

The second experiment was performed with fluorine atoms in Teflon-type plastic samples of thickness 0.6 and 1 mm. To facilitate the separation of the resonances from the background, a self-indication method was additionally used, i.e., for each of the angles 37, 87, and 140° an additional measurement was made with a Teflon-type plastic filter of thickness 2.4 mm in the beam. One of the pairs of spectra without the filter (black circles) and with the filter (open circles) is shown in the upper part of Fig. 9; then come the spectra without the sample and, in the bottom part, the difference of the upper spectra. It can be seen that the peaks are completely separated from the background (dashed curve)

TABLE I.

Target nucleus	Spin of nucleus I	Energy of resonance, keV	Spin of resonance J	Mixing parameter β	Reference
^{19}F	1/2	49.1	1	0.33±0.14	25
	I	97.0	1	0.33±0.13	
^{35}Cl	3/2	0.398	2	~0	31
^{89}Y	1/2	2.61	1	0.94±0.03	26
		3.38	1	0.90±0.04	
		9.41	1	0.62/0.05±0.05	
		12.99	1	0.62/0.04±0.04	
		14.21	(1)	0.83±0.06	
		20.27	1	0.85±0.11	
		23.00	1	0.64/0.03±0.04	
		24.56	1	0.58/0.09±0.06	
		29.26	1	0.96±0.05	
		30.05	1	0.79±0.03	
^{93}Nb	9/2	0.0358	5	0.30±0.08	21
		0.0422	4	0.73±0.17	
^{111}Cd	1/2	0.0045	1	0.67±0.07	22
^{113}Cd	1/2	0.0070	1	0.16±0.07	22
^{117}Sn	1/2	0.0013	1	0.82±0.08	22

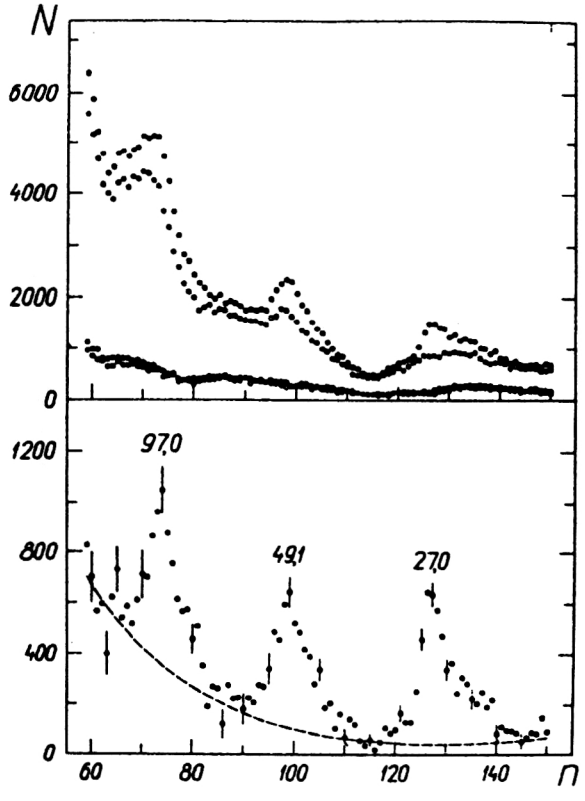

FIG. 9. Spectra for CF_2 sample of thickness 1 mm at angle 37°. The number of counts in the channel is N, and n is the number of a channel of width 1 μs. The numbers next to the peaks are the energies of the resonances in kilo-electron-volts.

fitted using the points outside the resonances. The result of this experiment[25] was again unexpected: For two resonances with $J=1$ (49.1 and 97.0 keV), ω_2 was found to be zero and $\beta \simeq 0.3$ (see Table I).

The third experiment was performed with the flight path of 1000 m and again with ^{89}Y nuclei. Around detector 1 (see Fig. 7) there were placed 16 thin aluminum containers filled with Y_2O_3 powder of total weight ~7 kg. Because the energy resolution, down to 30 keV, was better than in the first experiment with Y by a factor 4, 12 out of 25 known p-wave resonances could be "seen." Figure 10 shows extreme examples of peak separation: a) unresolved; b) weakest; c)

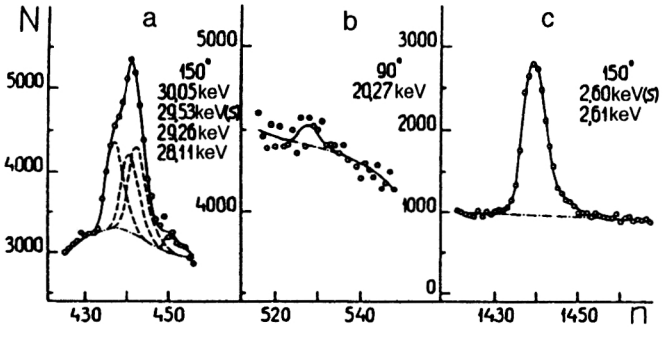

FIG. 10. Examples of fitting of ^{89}Y peaks for the indicated energies and angles.

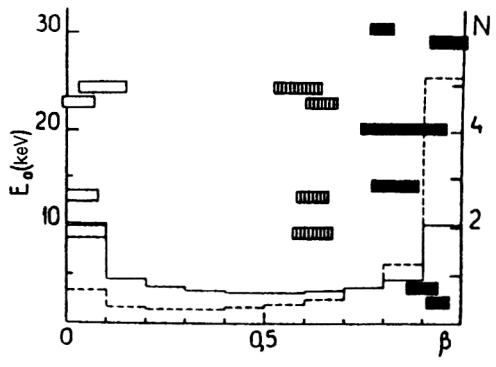

FIG. 11. Distribution of the values of β of ten ^{89}Y resonances. The values of N correspond to the histograms for the distribution (15) and indicate how many of the β values out of the ten must fall in the given interval of width 0.1.

strongest (of the p-wave resonances). The results are shown graphically in Fig. 11 (Ref. 26). Along the horizontal axis, the values of β are represented by the centers of the rectangles as a function of the resonance energy (left-hand ordinate), while the errors in β are indicated by the halves of their horizontal dimensions. Since $\omega_2 < 0.5$ for four resonances, it follows, in accordance with (17) for $J=1$ and Fig. 5, that their β can each have two values, which are shown by the open and hatched rectangles. The black rectangles are those with uniquely determined values of β.

To compare the observed distribution with the theoretical distribution (15), we have also plotted in Fig. 11 two histograms that show how many of the resonances out of the ten (along the right-hand scale) should have values of β within the given interval of width 0.1. Unfortunately, definite conclusions could be drawn from this comparison only under the two extreme assumptions of "two-valued" resonances. If all four resonances have smaller β, i.e., if there are no hatched rectangles in the figure, then the result of the experiment is consistent with a symmetric distribution (the solid continuous curve) corresponding to the absence of correlations between $\Gamma_{n+}^{(1)}$ and $\Gamma_{n-}^{(1)}$ that have Porter–Thomas fluctuations with equal mean values. If, however, the four resonances have larger β, i.e., if there are no open rectangles, then the black rectangles together with the hatched ones are concentrated in the interval $0.5 < \bar{\beta} < 1$, and this is extremely improbable (~0.2%) for a symmetric distribution. To explain this case, it is necessary to assume either a large difference of the mean widths [for the dashed histogram $\langle \Gamma_{n-}^{(1)} \rangle = 10 \langle \Gamma_{n+}^{(1)} \rangle$] or a strong correlation between the channels.

At the present time, we possess mixtures of spin channels for 18 p-wave resonances of seven nuclei. They are given in Table I and are clearly insufficient for a definite conclusion about correlations to be drawn. Nevertheless, the coincident β of ^{19}F and the same large β of four ^{89}Y resonances (if they are real) can be regarded as some indication in support of correlations. So can the following consideration in terms of the quotation from Shapiro given above.[6] For statistical independence of the widths in the different channels, one requires not only a high complexity of the wave functions of the compound states but also that the channel

wave functions be different. However, are different wave functions of the spin channels sufficient? In fact, they have completely identical spatial parts and differ only in the values of the spin variables. This difference may be insufficient for independent fluctuations of the corresponding overlap integrals with the resonance states, especially since hitherto there have been no experimental indications of any important role of spin–spin interaction in complex nuclei.

Concluding the discussion of the problem of spin channels in neutron resonances, we cannot fail to mention, at least briefly, the significant successes in the investigation of the analogous problem for proton resonances. At the University of Durham (USA), an investigation of six nuclei from ^{44}Ca to ^{56}Fe determined partial widths with the relative signs of the amplitudes for the exit proton channels (spin and orbital) in the p- and d-wave resonances of the $(p,p'\gamma)$ reaction.[27] In many tens of resonances, there were observed to be strong correlations in the magnitude and (or) in the sign for different pairs of channels in cases of the manifestation of isobar analog states and an appreciable contribution of the direct reaction mechanism. In addition, data were also obtained on spin channels in the elastic scattering of protons by nuclei with nonzero spin, i.e., data completely analogous to the neutron data discussed above. For the nuclei ^{25}Mg (Ref. 28), ^{27}Al (Ref. 29), and ^{29}Si (Ref. 30), between 6 and 15 resonances at the same spin were investigated for each nucleus. The results are consistent with purely statistical assumptions.

4. OBSERVATION OF SPIN–ORBIT SPLITTING OF STRENGTH FUNCTIONS

In this and the next two sections, we review experiments on the measurement of the differential cross sections $\sigma(\theta)$ of elastic scattering averaged over resonances. The idea of these experiments, which were performed under the direct influence of Shapiro, is most fully justified in Ref. 5; they began in 1982 (Ref. 32) and continued up to 1993 (Ref. 33) with the facility shown in Fig. 6. The bulk of the results and the complete employed mathematical basis are described in detail in our review of Ref. 17, and therefore we restrict ourselves here to merely a sketch of the idea and a listing of the results.

In Fig. 12, the symbols show the experimental values of the parameters in the three-term representation of the mean $\sigma(\theta)$ in accordance with (4) for cadmium nuclei, and the solid continuous curves show the best description of the experiment by a set of five parameters that determine the resonance and potential scattering of s- and p-wave neutrons. The advantages and shortcomings of the method can be deduced from the contributions to σ_s, ω_1, and ω_2 of the different components shown by the dashed curves. The main advantage is that up to an energy ~50 keV the values of ω_2 are almost completely determined by the $p_{3/2}$ component of the neutron strength function $S^1=(S^1_{1/2}+2S^1_{3/2})/3$, while the values of ω_1 at all energies are determined by the phase-shift ratio δ_1/δ_0 with small corrections for the resonances. As a result, two out of the five parameters are well determined ($S^1_{3/2}$ and δ_1), while the remaining three ($S^1_{1/2}$, S^0, and δ_0) are

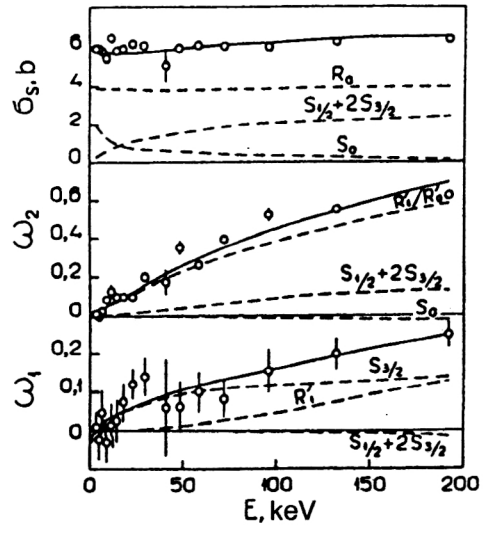

FIG. 12. Contributions of the different parameters to the formation of $\sigma(\theta)$ for cadmium nuclei.

somewhat less well determined on account of the correlations.

The many years of investigation of the p-wave strength function S^1 led, after disputes and errors (see, for example, Ref. 34), to an understanding of the fact that the $S^1_{1/2}$ and $S^1_{3/2}$ peaks are displaced on the scale of A by an amount ΔA that is less than their widths ~25–30. If the spin–orbit potential of the nucleus–neutron system is the same as in the shell model, ΔA should be ~5–8. The first report of separate observation of the $S^1_{1/2}$ and $S^1_{3/2}$ peaks, for 17 nuclei, was published in Ref. 35, and these peaks, augmented by the investigations of 14 more nuclei,[36–38] are represented in Fig. 13. The dashed curves show the result of describing the peaks by Lorentzian curves; this gave $\Delta A=13\pm4$, a value

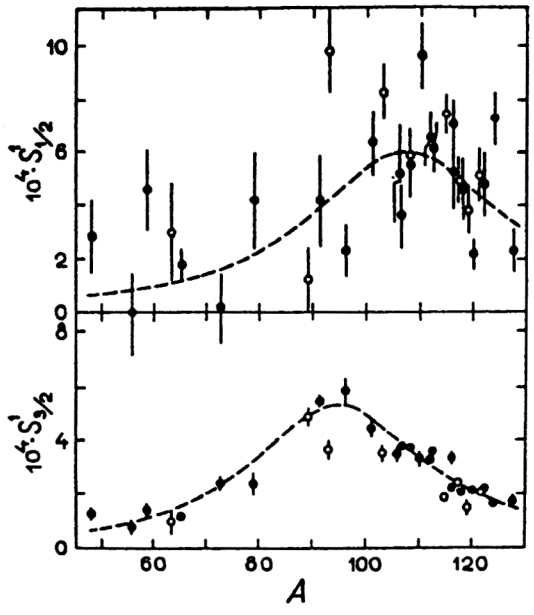

FIG. 13. Results on S^1_j for 22 even–even nuclei (black symbols) and 9 odd nuclei (open symbols).

that may be 1.5–2 times greater than it should be in the case of the widely accepted strength of the spin–orbit splitting of coupled single-particle levels.

This last circumstance, together with the properties of p-wave potential scattering (see Sec. 5), prompted the authors to make a theoretical analysis of their experimental results using the nuclear optical model.[39,40] The potentials from Refs. 18, 41, and 42 were tested, and for a spin–orbit component $V_{so}=7$ MeV they all gave $\Delta A\simeq 6$. An acceptable description of the positions of the peaks was obtained only for $V_{so}\simeq 10$ MeV. The calculations also showed that the "pure" optical model cannot make the $S^1_{1/2}$ peak higher than the $S^1_{3/2}$ peak, as is observed in the experiments.

Promising results were obtained by using a generalized optical model—a multiphonon version of the coupled-channel method.[43] In this model, the A-dependent coupling of the single-particle states with the collective 2^+ states (phonons) enabled the authors to reproduce reasonably well both the splitting and the heights of the $S^1_{1/2}$ and $S^1_{3/2}$ peaks with the generally accepted value of the spin–orbit potential.

5. DETERMINATION OF p-WAVE SCATTERING RADII

At high energies of the scattered particles, the phase shifts δ_l are unknown functions of the energy, and they are entirely determined from the experimental data. At low energies, when the wavelength of the incident particle is appreciably greater than the diameter of the nucleus, the phase shifts have a simple dependence on the energy and can be parametrized in the complete investigated range of energies by one or two parameters. In the investigations to be described, the R-matrix representation of the phase shifts was adopted:[17]

$$\delta_0=\phi_0+\sin^{-1}(kRR_0^\infty),\quad \phi_0=-kR,$$

$$\delta_1=\phi_1+\sin^{-1}\frac{(kR)^3R_1^\infty}{1+(kR)^2},\quad \phi_1=-kR+\tan^{-1}(kR), \tag{18}$$

where the channel radius is $R=1.35A^{1/3}$ F, and R_l^∞ is the parameter of the contribution of the more distant levels, which usually lies in the range from -0.4 to 0.4.

In discussions of neutron scattering, Shapiro often used the expression "radius of p-wave scattering," and in Ref. 5 he even introduced the notation R_1' for it. However, a rigorous definition of R_1' was given later[44] and follows from the proportion

$$\frac{R_l'}{R}=\lim_{E\to 0}\frac{\delta_l}{\phi_l},$$

whence

$$R_0'=R(1-R_0^\infty),\quad R_1'=R(1-3R_1^\infty). \tag{19}$$

The notation R_0' was long used (in the form R'), while R_1' was introduced only after Ref. 44.

The entire information known up to 1990 about R_1' (except for some points for $A<127$ in Ref. 41) is given in fermis in Fig. 14 in the dependence on A. The squares show the results that we obtained by means of (18) and (19) from

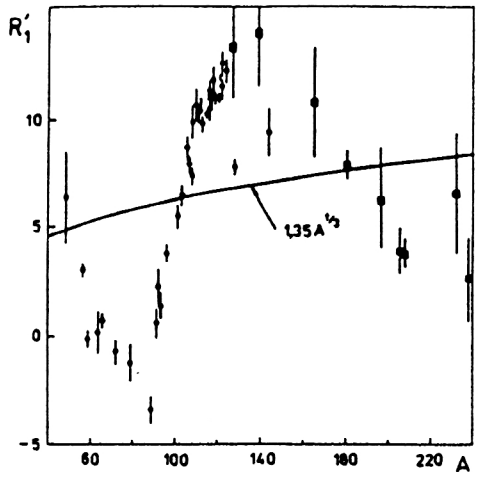

FIG. 14. Experimental values of R_j' in fermis.

studies in which high-precision measurements of the total cross sections at energies of hundreds of kilo-electron-volts were made. In these studies, the values of δ_1 were found either from the residue $12\pi\sin^2\delta_1/k^2$ of the cross section after the subtraction from it of the s-wave contribution[41] or from the interference of the resonance and potential p-wave scattering.[45–47] The remaining points in the figure were obtained in Dubna from the averaged $\sigma(\theta)$.

We note three features of the presented results. The main one is that the dependence $R_1'(A)$ is entirely similar to the long-known dependence $R_0'(A)$. Indeed, we see in the figure approximately one and a half periods of "modulation" of a monotonic function $\sim A^{1/3}$ by the oscillating quantity $1-3R_1^\infty$. The "modulation depth" is three times as large as in the case of the s wave and leads to very small and even negative values of R_1' for the nuclei with $A=60$–90; this is the second feature of $R_1'(A)$. The third feature is the downward excursion of $R_1'=8.1\pm 0.2$ F for Te by almost 20 standard deviations.

To establish more accurately the nature of these last two features, measurements were made with four further samples. Initially,[48] these were krypton and xenon gases in cylindrical containers of diameter 10 cm under a pressure of about 40 atm. Similar containers, one with oxygen and the other empty, were used to determine the absolute value of the cross section σ_s and take into account the background. The result for krypton ($A\simeq 84$) was $R_1'=-3.3\pm 1.2$ F and confirmed the "anomaly" of the radii for $A=60$–90, and for xenon ($A\simeq 131$) the result was $R_1'=10.6\pm 0.4$ F and confirmed the anomaly of the previously measured $R_1'\simeq 8$ F for tellurium averaged over the isotopes. Even more definite were the results[33] for the two enriched isotopes ^{128}Te (98.6%, 50 g) and ^{130}Te (99.6%, 50 g), for which $R_1'=6.2\pm 0.3$ and 6.3 ± 0.3 F, respectively, i.e., even lower than for Te.

A qualitative interpretation of the first two features in the behavior of $R_1'(A)$ was given in Ref. 17 on the basis of a rectangular potential well with gradually increasing imaginary part. Completely satisfactory agreement with the experiment was then obtained in optical-model calculations in both the simple[39,40] and generalized[43] forms. With regard to

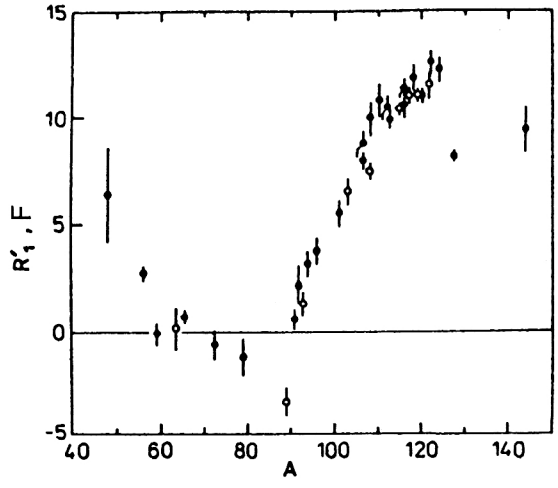

FIG. 15. Experimental values of the p-wave scattering radii. The black symbols are for even–even nuclei, and the open symbols for A-odd nuclei.

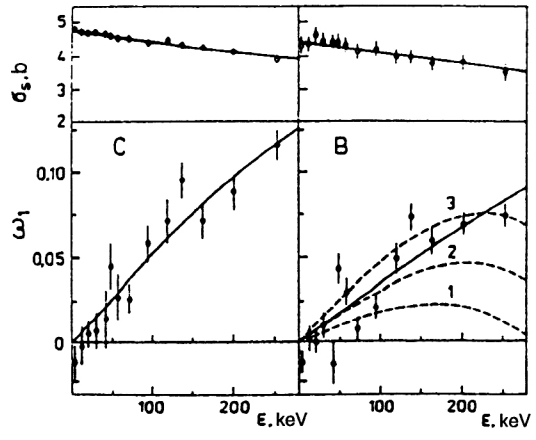

FIG. 16. Integrated cross section and scattering asymmetry (in the center-of-mass system). The points are the experimental results, and the curves are the theoretical description (see the text).

the tellurium anomaly, this manifestly nonstatistical effect was ascribed in Ref. 33 to doorway states in the ^{129}Te and ^{131}Te nuclei possessing spin $1/2^-$ or $3/2^-$ and corresponding to a neutron energy ~0.3 MeV.

6. ON ONE-PION EXCHANGE

Despite the huge successes of the quark–gluon description of hadrons, nuclei are at the least not very light, and at not too high energies they will probably still be regarded for a long time as neutron–proton systems in meson fields. The microscopic description of nuclear systems is based on the nucleon two-body interaction potential, which contains several terms corresponding to the different possibilities for nucleons to exchange one or several mesons of different species with different space–time properties. The effective interaction range for exchange of a given species and number of mesons is inversely proportional to the total mass of the exchanged mesons. Therefore, one-pion exchange has the greatest range, about 1.4 F. Exchanges of two pions or of more massive mesons give ranges less than 0.7 F.

Since the Hamiltonian of one-pion interaction contains as a factor the product of the spins of the interacting particles, the contribution of such exchange vanishes if one of the particles consists of paired nucleons with zero total spin. Therefore, in the interaction of a nucleon with a nucleus one-pion exchange is important only with an unpaired odd nuclear nucleon. All this indicates that when the neutron energies are not high and the peripheral p-wave interaction begins to be manifested the difference between the p-wave scattering radii on an odd and on a neighboring even–even nucleus will be to a large degree determined by the contribution of one-pion exchange.

Investigations were made of 19 nuclei (Refs. 44, 49, and 50; see also Ref. 17), the ω_1/E values of which apparently indicated an effect up to ~10% for an odd proton and the absence of an effect greater than 5% for an odd neutron. The final word in these searches was the study of Ref. 51, which was not included in Ref. 17 and from which a figure[4)] is reproduced here (Fig. 15). This cleaner and more reliable information about p-wave scattering permits the conclusion that the p-wave scattering radius of neutrons with energies up to 300 keV is barely subject to an influence of one-pion exchange greater than ~0.5 F for nuclei with $A \geqslant 90$. For lighter nuclei, this conclusion may be incorrect.

7. ON NEGATIVE p-WAVE RESONANCES

Strictly speaking, all compound-nucleus states with energy below the neutron binding energy and possessing spin differing from the target spin by $\pm 1/2$ or $\pm 3/2$ and a parity opposite to that of the target are negative p-wave resonances, and the only question about them is whether or not they are manifested in an experiment and what are their widths. Our assumption is that the parameters R_l^∞, being made up of a large number of "tails" of distant resonances, together with $R = 1.35A^{1/3}$ F give R_l' in accordance with (19), and these are nearly equal in magnitude for nuclei of nearly equal A, and that if they do differ appreciably, the difference should be ascribed to the effect of close resonances. In accordance with the coefficient of $\cos\theta$ in the expression (7) in Ref. 17 (see also footnote 3 in this paper), negative p-wave resonances give a positive correction to the "potential" ω_1, while positive resonances with energy greater than the given one make a negative correction.

In the studies of Refs. 52 and 53, measurements were made of $\sigma(\theta)$ in the representation (4) for beryllium, boron, and carbon at energies up to 250 keV. The experimental values of σ_s and ω_1 for two nuclei are illustrated by Fig. 16 (the results for Be are similar), and the values of the parameters R_l^∞ and R_l' extracted from the data for the three nuclei are given in Table II. We consider the figure first. The solid continuous curves in it are the result of fitting only by the parameters R_0^∞ and R_1^∞ for vanishing strength functions. For carbon this is correct, but for boron not completely so, since its ω_1 must be distorted by the close and strong p-wave resonance of ^{11}B at $E_0 = 430$ keV. Allowance for this resonance with the previously obtained $R_1^\infty = -0.003$ (and $R_1' = 3.0$ F) gives for the ω_1 of boron curve *1*, which is clearly unsatisfactory. However, the use of $R_1^\infty = 0.14$, as for carbon, which for boron gives $R_1' = 4.2$ F, leads to curve *2*, which is

TABLE II.

Element	R, F	R_0^∞	λ^*,keV^{-1}	R_1^∞	R_0', F	R_1', F
Be	2.81	−1.44(3)	$9(3)\cdot10^{-4}$	−0.47(4)	6.85(9)	6.75(33)
B	2.99	−0.99(3)	$4(3)\cdot10^{-4}$	−0.27(3)	5.95(10)	5.38(28)
C	3.09	−0.99(1)	$2.5(6)\cdot10^{-4}$	−0.14(3)	6.15(2)	4.38(24)

still below the majority of the points. Curve *3* is good; for it, $R_1^\infty=0.27$, while $R_1' = 5.4$ F is already appreciably larger than for carbon (see Table II). Therefore, our next steps were the following: Having fixed for boron and beryllium the value $R_1^\infty=-0.14$ (i.e., as for carbon), we described their ω_1 with direct allowance for one p-wave resonance with $E_0=-709$ keV (^{12}B 2720 keV, 0^+ level) for boron and two p-wave resonances with $E_0=-703$ and -949 keV (^{10}Be 6179 keV, 0^+ and 5958 keV, 2^+ levels) for beryllium in accordance with Ref. 54. This led to the following estimates for the reduced neutron widths of the p-wave resonances:

$$\Gamma_n^{(1)}(-709 \text{ keV}, J=0^+)\simeq 4.0 \text{ keV} \quad \text{for } ^{11}\text{B}, \tag{20}$$

$$\Gamma_n^{(1)}(-703 \text{ keV}, J=0^+)+3.8\Gamma_n^{(1)}(-949 \text{ keV}, J=2^+)\simeq 7.5 \text{ keV} \quad \text{for } ^{9}\text{Be}, \tag{21}$$

which were found to be comparable with the Wigner limits $\Gamma_{n\text{W}}^{(1)}=6.1$ and 6.5 keV of the widths calculated from the single-particle width $\gamma^2=\hbar^2/(mR^2)$ for ^{11}B and ^{9}Be, respectively (m is the neutron mass).

Thus, for beryllium and boron we have two alternative descriptions of the experiment that are equivalent as regards their quality: one with the parameters in Table II and another that, in our view, is more realistic with the same $R_1^\infty=-0.14$ for all three elements and parameters (20) and (21) of the negative resonances.

8. PROSPECTS

In the investigations described above, which extended over 30 years, the anisotropy of neutron scattering at energies from a few to hundreds of kilo-electron-volts was measured for 30 elements and 16 enriched isotopes. However, many problems associated with p-wave neutrons were not so much solved as merely posed. This applies to the estimate of the neutron polarizability (Sec. 1), the determination of the spin-channel mixtures (Sec. 3), the interpretation of the tellurium anomaly with the p-wave scattering radii (Sec. 5), the elucidation of the contribution to p-wave scattering of one-pion exchange in nuclei with $A<90$ (Sec. 6), and the determination of the widths of negative p-wave resonances (Sec. 7).

It is hoped to resolve all these and, possibly, other problems at the Laboratory of Neutron Physics by means of the high-luminosity and low-background facility UGRA that is being developed.[55] The possibilities of this facility as regards the energy range and resolution will be significantly improved on the introduction of the new neutron source IREN. The arrangement of the facility is shown in Fig. 17. A low background is achieved by the fact that the collimated neutron beam, the investigated samples, and the neutron detectors are in a common vacuum region, and the walls of the vacuum chamber, which are far from the scatterers and de-

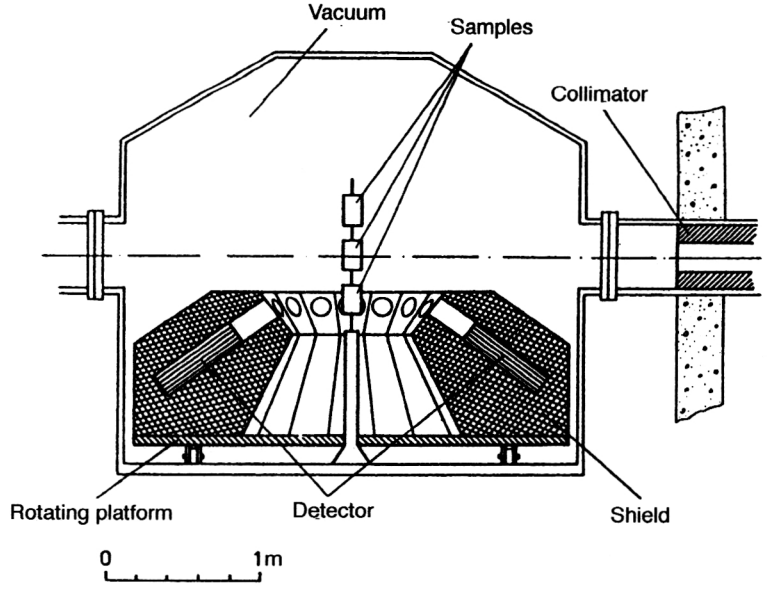

FIG. 17. Schematic arrangement of the UGRA facility that is being constructed.

tectors and have height and diameter ~3 m, reduce the effect of neutron rescattering by these walls (aluminum of thickness 12 mm). A high efficiency of the facility may also be ensured by the fact that it is designed for the use of 16 detectors equivalent to the one used in the facilities shown in Figs. 6 and 7 and employed in all the studies described in Secs. 3–7 (^{3}He detector, ~8 liter, ~10 atm). Mounted on a common rotating platform, each detector measures its "own" angular distribution of the scattering at angles from 30 to 150°.

The UGRA facility is being constructed with financial support by the Russian Fund for Fundamental Research (Project 93-02-17384) and the International Science Foundation (Grant RFS000).

[1)]In all the equations, the cross sections and their parameters are assumed to be expressed in the center-of-mass system and the energy E in the laboratory system; in connection with this, $k=0.00021968A\sqrt{E}/(A+1)\,F^{-1}$, *where* E is measured in electron volts.

[2)]In writing down the widths (14) and the scheme of addition of the angular momenta (13), we have used the spin-channel representation. It is very common to use the representation of the total angular momentum of the neutron, $\mathbf{j}=\mathbf{l}+\mathbf{1/2}$, and one then speaks of a mixture of p-wave neutron channels with $j=1/2$ and 3/2 (see, for example, Ref. 22).

[3)]We have here omitted the term $\omega_1 \cos\theta$ that arises from the second term of the expansion (1) describing the interference of p-wave resonance scattering with the s-wave potential scattering. The principal part of this term is an odd function with respect to the resonance energy and gives zero on integration within symmetric limits.

[4)]Unfortunately, in the caption to this figure in Ref. 51 the open and black symbols have been interchanged.

[1] A. A. Bergman, A. I. Isakov, M. V. Kazarnovskiĭ, I. D. Murin, F. L. Shapiro, and I. V. Shtranikh, in *Proceedings of the International Conference on the Peaceful Uses of Atomic Energy*, Geneva, 1955, Vol. 4 (United Nations, New York, 1956) [Russ. transl., Akademizdat, Moscow, 1957].
[2] A. Asami, M. C. Moxon, and W. E. Stein, Phys. Lett. B **28**, 656 (1969).
[3] Yu. P. Popov and Yu. I. Fenin, Zh. Éksp. Teor. Fiz. **43**, 2000 (1962) [Sov. Phys. JETP **16**, 1409 (1963)].
[4] F. L. Shapiro, *Collected Works. Neutron Physics* (Nauka, Moscow, 1976), p. 313.
[5] Yu. P. Popov and Yu. I. Fenin, in *Proceedings of the Working Symposium on the Interaction of Neutrons with Nuclei* [in Russian] (JINR-1845, Dubna, 1964).
[6] F. L. Shapiro, in *Collection of Lectures at the All-Union Summer School on Nuclear Spectroscopy in Nuclear Reactions*, July 3–19, 1966 [in Russian] (Physics and Power Institute, Obninsk, 1967), p. 239.
[7] A. Klein, Phys. Rev. **99**, 998 (1955).
[8] Yu. A. Aleksandrov and I. I. Bondarenko, Zh. Éksp. Teor. Fiz. **31**, 726 (1956) [Sov. Phys. JETP **4**, 612 (1957)].
[9] Yu. A. Aleksandrov, *Fundamental Properties of the Neutron* (Énergoatomizdat, Moscow, 1992).
[10] R. M. Thaler, Phys. Rev. **114**, 827 (1959).
[11] V. F. Sears, Phys. Rep. **141**, 281 (1986).
[12] Yu. A. Aleksandrov, D. Dorchoman, Zh. Séréétér, G. S. Samosvat, and Tsoĭ Gen Sor, in *Program and Abstracts of Papers at the 15th Annual Symposium on Nuclear Spectroscopy and Nuclear Structure*, Minsk, 1965 [in Russian] (Nauka, 1965), p. 83.
[13] M. D. Goldberg, V. W. May, and J. R. Stehn, BNL-400, 2nd ed. (1962).
[14] Yu. A. Aleksandrov, G. S. Samosvat, Zh. Séréétér, and Tsoĭ Gen Sor, Pis'ma Zh. Éksp. Teor. Fiz. **4**, 196 (1966) [JETP Lett. **4**, 134 (1966)].
[15] Yu. A. Aleksandrov and G. S. Samosvat, Preprint JINR R3-4354, Dubna (1969) [in Russian].
[16] G. S. Samosvat, Yad. Fiz. **11**, 1152 (1970) [Sov. J. Nucl. Phys. **11**, 639 (1970)].
[17] G. S. Samosvat, Fiz. Elem. Chastits At. Yadra **17**, 713 (1986) [Sov. J. Part. Nucl. **17**, 313 (1986)].
[18] P. A. Moldauer, Nucl. Phys. **47**, 65 (1963).
[19] A. M. Lane, Ann. Phys. (N.Y.) **63**, 171 (1971).
[20] R. C. Block, W. Haeberli, and H. W. Newson, Phys. Rev. **109**, 1620 (1958).
[21] R. E. Chrien, M. R. Bhat, and G. W. Cole, Phys. Rev. C **8**, 336 (1973).
[22] É. I. Sharapov, in *Fifth International School of Neutron Physics, Alushta, 1986*, D3,4,17-86-747 [in Russian] (JINR, Dubna, 1987), p. 113.
[23] V. P. Alfimenkov, V. N. Efimov, Ts. Ts. Panteleev, and Yu. I. Fenin, Yad. Fiz. **17**, 293 (1973) [Sov. J. Nucl. Phys. **17**, 149 (1973)].
[24] V. G. Nikolenko and G. S. Samosvat, Yad. Fiz. **23**, 1159 (1976) [Sov. J. Nucl. Phys. **23**, 616 (1976)].
[25] V. G. Nikolenko and G. S. Samosvat, in *Neutron Physics (Proceedings of the Fifth All-Union Conference on Neutron Physics, Kiev, 1980)*, Part 2 [in Russian] (Central Research Institute of Atomic Information, Moscow, 1980), p. 178.
[26] V. G. Nikolenko and G. S. Samosvat, Preprint JINR E3-82-336, Dubna (1982).
[27] G. E. Mitchell, E. G. Bilpuch, J. F. Shriner, Jr., and A. M. Lane, Phys. Rep. **117**, 1 (1985).
[28] G. Adams, E. G. Bilpuch, G. E. Mitchell, R. O. Nelson, C. R. Westerfeldt, J. Phys. G **10**, 1747 (1984).
[29] R. O. Nelson, E. G. Bilpuch, C. R. Westerfeldt, and G. E. Mitchell, Phys. Rev. C **29**, 1656 (1984).
[30] R. O. Nelson, E. G. Bilpuch, C. R. Westerfeldt, and G. E. Mitchell, Phys. Rev. **27**, 930 (1983).
[31] C. M. McCullagh, M. J. Kenny, and R. E. Chrien, Phys. Rev. C **19**, 539 (1979).
[32] V. G. Nikolenko, A. B. Popov, and G. S. Samosvat, in *Nuclear Data for Science and Technology (Proceedings of the International Conference, Antwerp)* (1982), p. 781.
[33] L. V. Mitsyna and G. S. Samosvat, Yad. Fiz. **56**, No. 2, 23 (1993) [Phys. At. Nucl. **56**, 159 (1993)].
[34] G. S. Samosvat, Communication R3-83-532 [in Russian] (JINR, Dubna, 1983).
[35] Zo In Ok, V. G. Nikolenko, A. B. Popov, and G. S. Samosvat, Pis'ma Zh. Éksp. Teor. Fiz. **38**, 304 (1983) [JETP Lett. **38**, 363 (1983)].
[36] Zo In Ok, A. I. Poplova, A. B. Popov, I. M. Salamatin, and G. S. Samosvat, Communication R3-84-668 [in Russian] (JINR, Dubna, 1984).
[37] A. B. Popov and G. S. Samosvat, in *Nuclear Data for Basic and Applied Science*, Vol. 1 *(Proceedings of the Conference, Santa Fe, 1985)*, p. 621.
[38] A. B. Popov and G. S. Samosvat, Yad. Fiz. **45**, 1522 (1987) [Sov. J. Nucl. Phys. **45**, 944 (1987)].
[39] L. V. Kuznetsova, A. B. Popov, and G. S. Samosvat, in *Neutron Physics. Proceedings of the First International Conference on Neutron Physics*, Kiev, 1987, Vol. 2 [in Russian] (Central Research Institute of Atomic Information, Moscow, 1988), p. 254.
[40] L. V. Mitsyna, A. B. Popov, and G. S. Samosvat, in *Nuclear Data for Science and Technology. Proceedings of the International Conference*, Mito, Japan, 1988 (JAERI, 1988), p. 111.
[41] H. S. Samarda, Phys. Rev. C **9**, 28 (1974).
[42] A. B. Smith, P. T. Guenther, and J. F. Whalen, Nucl. Phys. A **415**, 1 (1984).
[43] V. V. Samoĭlov and M. G. Urin, Yad. Fiz. **52**, 1325 (1990) [Sov. J. Nucl. Phys. **52**, 839 (1990)].
[44] Yu. A. Aleksandrov, G. G. Bunatyan, V. G. Nikolenko, A. B. Popov, and G. S. Samosvat, in *Neutron Physics (Proceedings of the Fifth All-Union Conference on Neutron Physics, Kiev, 1980)*, Part 2 [in Russian] (Central Research Institute of Atomic Information, Moscow, 1980), p. 163.
[45] D. J. Horen, J. A. Harvey, and N. W. Hill, Phys. Rev. C **18**, 722 (1978).
[46] D. J. Horen, J. A. Harvey, and N. W. Hill, Phys. Rev. C **24**, 1961 (1981).
[47] I. Tsubone and Y. Kanda, in *Nuclear Data for Science and Technology (Proceedings of the International Conference, Antwerp, 1982)*, p. 65.
[48] A. M. Govorov, L. V. Mitsyna, and G. S. Samosvat, Yad. Fiz. **54**, 1192 (1991) [Sov. J. Nucl. Phys. **54**, 723 (1991)].
[49] Yu. A. Aleksandrov, G. G. Bunatyan, V. G. Nikolenko, A. B. Popov, and G. S. Samosvat, Yad. Fiz. **32**, 1173 (1980) [Sov. J. Nucl. Phys. **32**, 605 (1980)].
[50] Yu. A. Aleksandrov, V. G. Nikolenko, A. B. Popov and G. S. Samosvat, Communication R3-81-432 [in Russian] (JINR, Dubna, 1981).
[51] L. V. Kuznetsova, A. B. Popov, and G. S. Samosvat, Communication R3-87-114 [in Russian] (JINR, Dubna, 1987).

[52] L. V. Mitsyna, A. B. Popov, and G. S. Samosvat, Pis'ma Zh. Éksp. Teor. Fiz. **49**, 248 (1989) [JETP Lett. **49**, 281 (1989)].
[53] D. I. Lyapin, L. V. Mitsyna, A. B. Popov, I. M. Salamatin, and G. S. Samosvat, Communication R3-89-408 [in Russian] (JINR, Dubna, 1989).
[54] *Table of Isotopes*, edited by C. M. Lederer and V. C. Shirley (New York, 1978).
[55] Yu. A. Aleksandrov and G. S. Samosvat, in *Sixth International School of Neutron Physics*, Alushta, 1990, D3,14-91-154 [in Russian] (JINR, Dubna, 1991), p. 187.

Translated by Julian B. Barbour